Organic/Inorganic-Polyimide Nanohybrid Materals for Advanced Optical Applications

Shinji ANDO

Department of Chemistry & Materials Science, Tokyo Institute of Technology, Ookayama 2-12-1, Meguro-ku, Tokyo 152-8552, JAPAN

Tel: +81-3-5734-2137, Fax: +81-3-5734-2889, E-mail: sando@polymer.titech.ac.jp

Abstract : Nano-hybridization techniques based on the pyrolytic reactions of organo-soluble metallic precursors dissolved in poly(amic acid)s followed by spontaneous precipitation of metal/inorganic nanoparticles in solid polyimide(PI) films is a facile and very effective technique for the functionalization of PI optical materials. The organic/inorganinc PI nanohybrid materials, which were recently developed by the authors, having optical functionalities, such as *a*) high refractive indices, *b*) low refractive indices, *c*) controlled thermo-optical property and its anisotropy, and *d*) high polarizing property, are reviewed with the overviews and future prospects on their industrial applications.

Introduction

The advantages of polymers in the application to optical components, such as micro-lens for CCD/CMOS image sensors, thin films and anti-reflective coatings for flat-panel displays (LCD and OLED), and waveguide circuits in optical interconnects and telecommunications (Scheme 1), are *1*) facile formation of thin films at lower temperatures, *2*) light-weight, toughness, and flexibility, *3*) micro-patternability by phtolithography or imprinting, *4*) wide range of molecular design, and *5*) facile incorporation of metallic or inorganic dopants or nanoparticles.[1–5] In contrast, the drawbacks of polymeric materials are *a*) low thermal stability, *b*) high moisture absorption, *c*) low environmental stability and durability, and *d*) narrow range of controllable optical properties such as transmittance, wavelength range with high transparency, refractive indices, birefringence, and thermo-optic coefficients. Recently, with the rapid development of nanoscience and nanotechnology, various methods to provide functional optical polymers have been revealed. In particular, nano-hybridization of optical polymers with metallic or inorganic nanoparticles is a promising technique to overcome the drawbacks without reducing their inherent advantages.[6–8] When the sizes of nanoparticles are smaller than 40 nm (~1/10 of the visible wavelengths), nanohybrid films are in general transparent. The sol-gel method, which is a wet-chemical process for the fabrication of metal oxide starting from a organic solution undergoing hydrolysis and polycondensation reactions followed by drying and thermal curing for further condensation and consolidation, is a promising technology. Since the sol-gel process uses organo-soluble compounds as source materials, it can afford metal oxide, such as SiO_2, ZrO_2, ZnO, TiO_2, Al_2O_3, at much lower temperatures than thermal fusion method. In addition, polyimides (PIs) are generally cured at higher temperatures (250~400°C) than conventional optical polymers, wider range of precursors can be used as the source materials for metallic and inorganic nanoparticles.

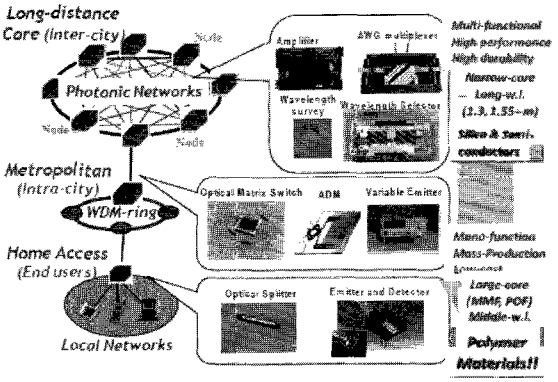

Scheme 1. Hierarchic structure of optical networking systems and optical components used therein.

安藤 慎治 (あんどうしんじ) : 東京工業大学大学院 理工学研究科 物質科学専攻

Highly Refractive PIs[9–18] : High refractive index (high-n) and low birefringence (Δn) combined with good thermal stability and high transparency are the basic concerns in designing polymer coatings for micro-lens applications. According to the Lorentz-Lorenz equation (1)[9], conventional polymers could be endowed with high refractive indices by introducing substituents having higher molar refraction and lower free molecular volumes. In particular, sulfur-containing substituents are one of the most promising candidates. Scheme 2 shows the sulfur-containing PIs reported by Liu and Ueda.[9–16] The optical absorption spectra and the refractive index dispersions of the PIs derived from APTT diamine are shown in Fig. 1. The PI (3SDEA-APTT) with the highest sulfur content of 23.2 % shows the highest n of 1.761 at 632.8 nm. This is one of the top values in high-n polymers. The experimental absorption edges agree well with the calculated values by TD-DFT method[19–23], and the refractive index dispersions are well fitted by the simplified Cauchy's formula ($n_\lambda = n_\infty + D/\lambda^2$). The n_∞ reflects the inherent refractive index of a PI, which is not influenced by electronic absorptions. Figure 2 shows the relations between the values of n_∞ and D. Two different linear relationships are observed for the semi-alicyclic and aromatic PIs, which agree well with the relation that we have reported previously.[24] The higher the n_∞, the larger the D, which straightforwardly indicates that a high-n rarely exists with a low D. Among various dianhydrides, ODPA and mDPSDA, which have lower electron affinities, can provide PIs with higher transparency and lower dispersion. PI (CHDA-APTT) exhibits the highest optical transparency with n=1.680 and Δn=0.0048. Thus, it was combined with SiO_2-modified TiO_2 nanoparticles.[13] The PAA solution showed good affinity with nanoparticles up to the proportion of poly(amic acid) (PAA):TiO_2=55:45 (w/w), and a homogeneous mixture was readily achieved using a mechanical stirrer.

$$\frac{n_\lambda^2 - 1}{n_\lambda^2 + 2} = \frac{4\pi}{3} K_p \frac{\alpha_\lambda}{V_{vdw}} \quad (1)$$

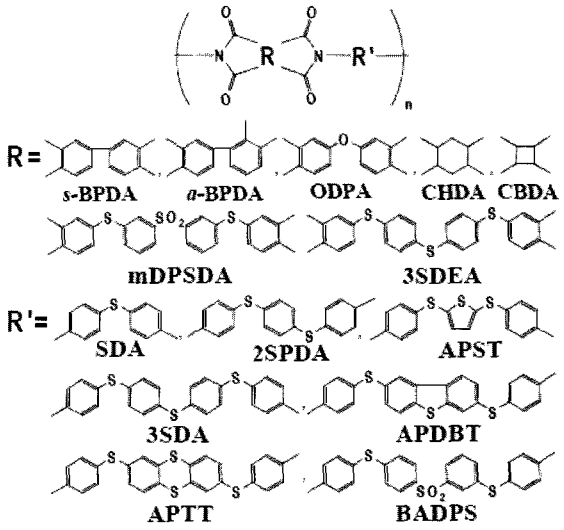

Scheme 2 Molecular structures of sulfur-containing PIs exhibiting high refractive indices.

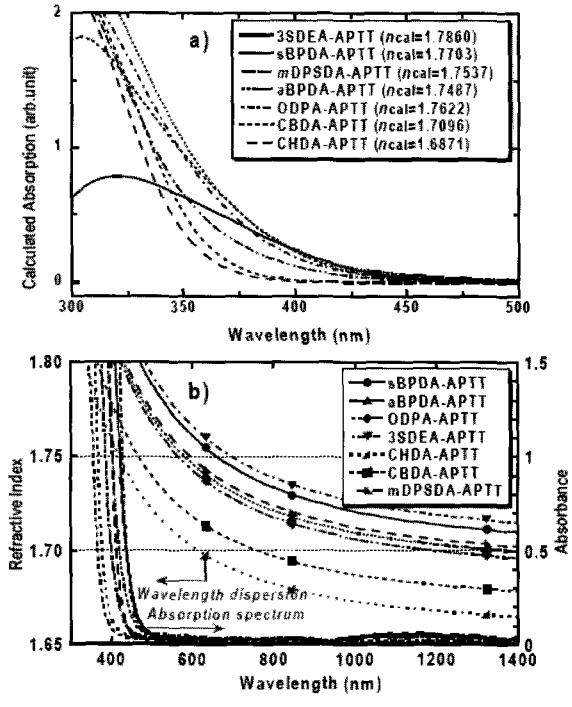

Fig.1 a) Calculated absorption spectra with calculated refractive indices (*inset*), and b) experimental absorption spectra and wavelengths dispersion of refractive indices of the PI films derived from APTT diamine.

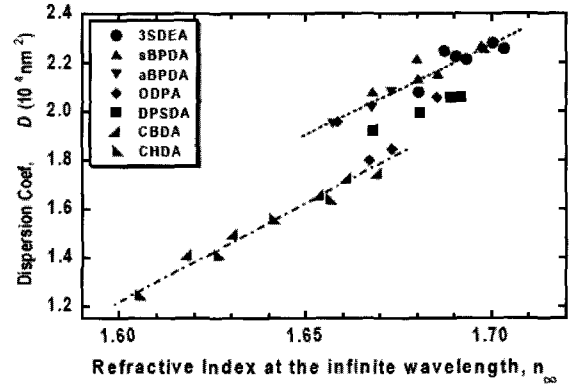

Fig.2 Relations between the n_∞ values and the dispersion coefficients (D) for the PIs derived from 7 kinds of dianhydrides.

The homogeneous and transparent film has a very high refractive index of 1.810 at 632.8 nm, which achieves the target (n >1.80). This value could be evaluated from the equation; $n_{hyb}=\phi_{par}\cdot n_{par}+\phi_{pol}\cdot n_{pol}$ (n_{hyb}, n_{par}, and n_{pol} are the refractive indices of nanohybrid, particle, and polymer matrix, respectively, and ϕ_{par} and ϕ_{pol} are the volume fractions of nanoparticles and matrix) with the parameters of ρ_{par}=3.11, n_{par}= 2.00, ρ_{pol} = 1.45, and n_{pol}=1.68. The estimated n_{hyb} value (~1.78) is slightly lower than that of the experimental n_{hyb}, which might be attributable to the densification of PI nanohybrid films due to the interactions between the PI chains and the modified TiO_2 surfaces.

Lowly Refractive PIs[25] : Low-n materials also have a high demand for anti-reflective coatings and OLED applications. We have been developing PIs exhibiting high transparency with low refractive indices by introducing fluorines and alicyclic structures in the main chain (Scheme 3).[26] The PI (6FDA-DCHM) shows a low n of 1.509 with a low Δn of 0.001 at 1324 nm. We attempted to lower the n of PI by incorporating magnesium fluoride (MgF_2) nanoparticles. MgF_2 is known as a representative low-n inorganic glass with a refractive index of 1.38 at 633 nm. Since $Mg(CF_3COO)_2{\cdot}nH_2O$ (MgTfAc) was reported to be thermally converted to MgF_2 under nitrogen at ca.300°C recently.[27] MgTfAc was dissolved in a DMAc solution of PAA of 6FDA-DCHM to afford a precursor for PI nanohybrid. Figure 3 shows the ^{19}F magic-angle spinning (MAS) NMR and Fourier-transformed (FT) far-infrared (Far-IR) absorption spectra of the hybrid films thus obtained, which demonstrate that 93.3% of MgTfAc was converted to MgF_2 by curing at 300°C, but MgTfAc was unchanged at 200 and 250°C despite the complete imidization of PAA at 200°C. The hybrid films cured at 200 and 250°C are perfectly colorless and transparent, which is same as the pristine PI film. In contrast, the hybrid film cured at 300°C show pale-yellow color with slight haze due to the light scattering caused by precipitated MgF_2 nanoparticles. Since amorphous MgF_2 crystallizes over 600°C,[27] no diffraction peaks characteristic to MgF_2 were observed in the WAXD patterns of all films. Figure 4 shows the curing temperature dependence of the refractive indices of the PI nanohybrid films prepared with different MgTfAc contents. The observed n values were systematically reduced by –1.5, –1.6, –0.75 % by the incorporation of MgTfAc to the PIs cured at 200, 250 and 300°C, respectively, at 100 mol% of MgTfAc content. Since MgTfAc was not decomposed in the PI films at 200 and 250°C, the n values of these films are proportional to the MgTfAc content. Note that the n values of these films are significantly lower than those of the films cured at 300°C. MgTfAc was unchanged in the former but decomposed to MgF_2 in the latter, which indicates that the inherent refractive index of MgTfAc is much lower than MgF_2. This is explain-

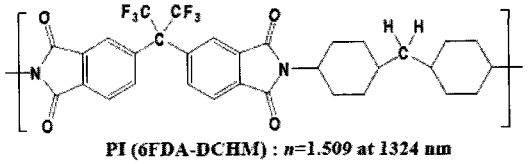

Scheme 3 Structure of a semi-alicyclic fluorinated PI exhibiting low n and low Δn.

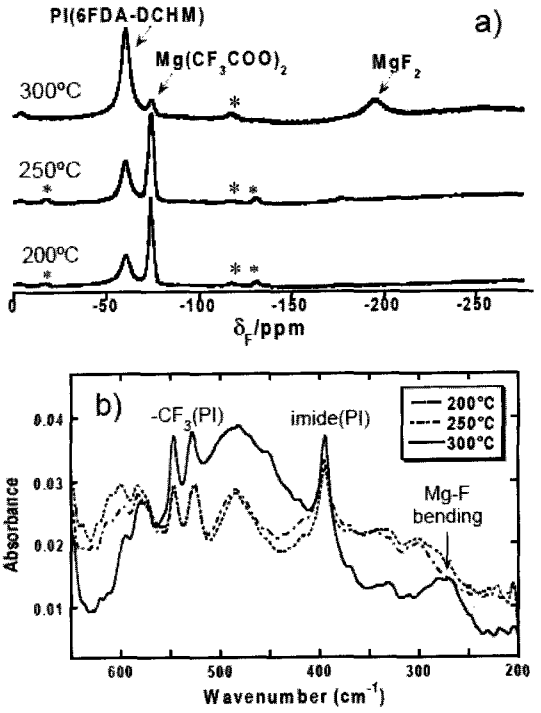

Fig.3 a) ^{19}F MAS and b)FT-FarIR spectra of PI (6FDA-DCHM) films with MgTfAc (100 mol%) cured in vacuo at 200, 250, and 300°C.

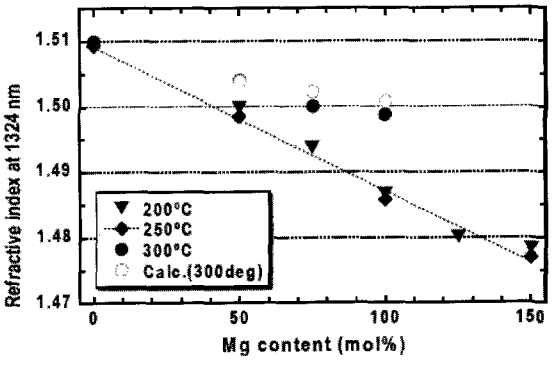

Fig.4 Refractive indices of PI (6FDA-DCHM) films with different amounts of MgTfAc cured at 200, 250, and 300°C. The open circles indicate the calculated refractive indices using the n of MgF_2.

able by the fact that the molar ratio of Mg to F is 1 : 6 for MgTfAc and 1 : 2 for MgF_2.

PIs with Controled Thermo-optic Coefficients[28–32]: The temperature dependence of refractive indices ($|dn/dT|$) of polymers, which is called 'thermo-optic coefficients', are significantly larger than those of inorganic glasses because polymers possess much larger thermal expansion. Hence, optical polymers are suitable for the materials for thermo-optical switches and wavelength-selective arrayed waveguide (AWG) filters. In order to achieve a larger $|dn/dT|$, a higer refractive index and/or a larger thermal expansion are required. Introduction of sulfur atoms or aromatic rings are effective for the former, and an increase in free volume is significant for the latter. We have demonstrated that the introduction of siloxane linkages in the main chain of PIs effectively lower the glass transition temperature (T_g) to 60°C, and the values of $|dn/dT|$ can be increased to 350 ppm/K[31] (typical values below T_g are ca.70-100 ppm/K). In addition, the application of sol-gel process using tetraethoxysilane (TEOS) as a silica (SiO_2) source successfully endows good solvent resistivity to the PIs. The introduction of SiO_2 by 10 wt% significantly raises the T_g, which simultaneously enables to control the $|dn/dT|$. Although PI/silica nanohybrids seems to exhibit smaller $|dn/dT|$ due to the formation of silica networks, an apparent increase in $|dn/dT|$ was observed at lower SiO_2 contents, and then turned to decrease at higher SiO_2 contents. A similar tendency was observed for the polarization anisotropy in $|dn/dT|$, which corresponds to the temperature dependence of in-plane/out-of-plane birefringence (Δn). We have clarified that these parameters are proportional to the thermal expansion coefficients along the out-of-plane direction ($\alpha_\perp$) (Fig.6) These facts indicates that, at lower silica contents, volume thermal expansion is instantly increased due to the increase in free volumes between PI chains and nanoparticles. Since PI films are formed on silicon substrates, in-plane thermal expansion is suppressed, and vertical (out-of-plane) expansion is enhanced, which is the reason of the simultaneous increases in $\alpha_\perp$, $|dn/dT|$, and $|d(\Delta n)/dT|$. In contrast, at higher silica contents, the thermal volume expansion is effectively suppressed by the growing silica networks which effectively reduce the $|dn/dT|$, and $|d(\Delta n)/dT|$.

Thin Film PI Polarizer[32–37]: Linear polarizing films made of poly(vinyl alcohol) films dyed with iodine are widely used for liquid crystalline displays (LCDs), but this type of films cannot be used for optical communication applications because iodine does not exhibit anisotropic absorptions in the near-infrared (NIR) region. Instead, inorganic polarizer fabricated by uniaxial elongation of

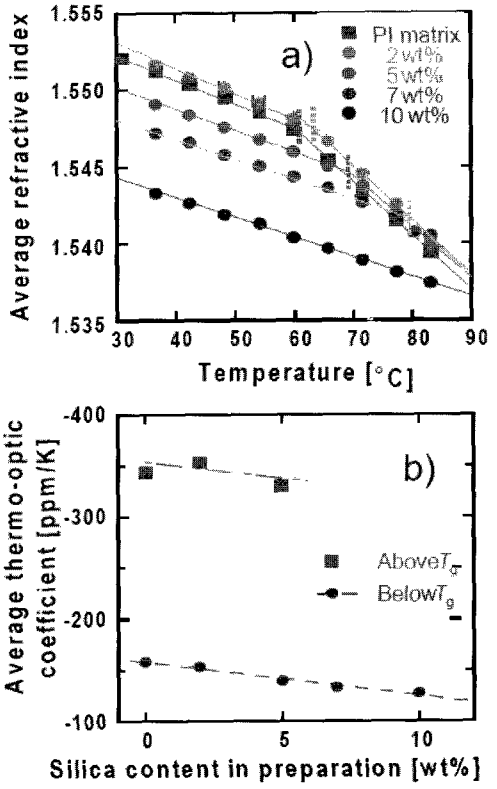

Fig.5 a) Temperature dependence of n_{av} of PI/silica nanohybrid films, and b) the silica-content dependence of dn_{av}/dT for the hybrid films below and above T_g.

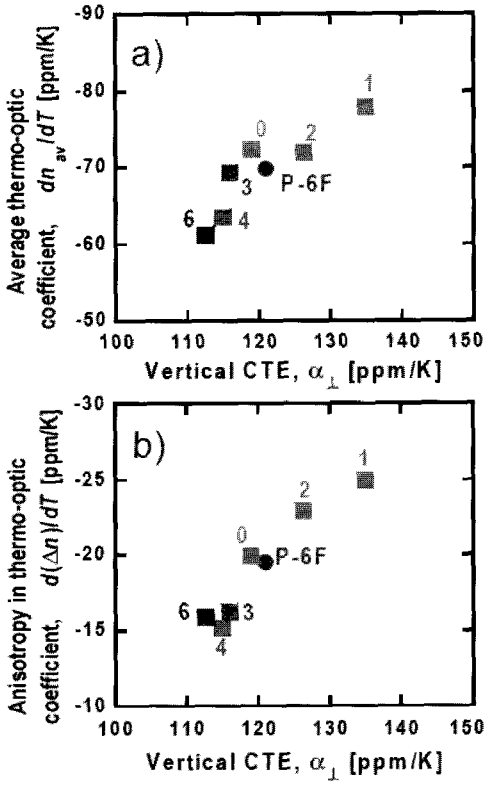

Fig.6 Relationships between the thermal expansion coefficients along the out-of-plane direction (vertical CTE, $\alpha_\perp$) and a) $|dn/dT|$ and b) $|d(\Delta n)/dT|$ in silica-PI nanohybrids.

silver or copper nanoparticles dispersed in inorganic glasses are used in fiber-optic devises such as optical isolators. Metal nano-rods show significant polarizing properties in the visible-NIR regions, though glass matrix have drawbacks in the thickness (150~200 μm), fragility, processability, and mass-production. Hence, we tried to fabricate thin film polarizers based on silver nanoparticles dispersed in colorless and transparent PIs having rigid-rod structures. A new series of copolymers consisting of a sulfur-containing PAA having high affinity to noble metals and a fluorinated PAA having low affinity were prepared, and silver nitrate was dissolved in a DMAc solution of the PAA. Due to the large difference in hydrophobicity between the two components, the dried PAA films exhibited typical micro-phase separation, and energy dispersive spectroscopy (EDS) clarified that nanometer-sized silver particles were selectively concentrated and precipitated in the sulfur-rich domain. During simultaneous curing and uniaxial drawing at higher temperatures (>350°C), the PI films showed apparent polarizing properties in the visible-NIR regions due to the deformed shapes of silver nanoparticles. Since it has been reported that the melting temperatures (T_m) of metal nanoparticles are significantly lower than those of bulk (T_m of bulk silver is 689°C), such nanoparticles can be elongated at appropriate conditions (temperature, atmosphere, and tensile stress). We developed a new apparatus for the *in-situ* and *real-time* observation of polarized transmission spectra to monitor and control the temperature and drawing conditions. The silver nano-rods thus precipitated in the copolyimide film show significantly elongated shapes (50 ×300 nm) with perfect orientation along the drawing direction (Fig. 7). The WAXD pattern of the film shows that these particles are nano-crystallites of zero-valent silver, and the PI film thus obtained shows very good polarizing property (dichroic ratio: >500 at 1550 nm) with high optical transmission (>70 %) (Fig. 8). In addition, the PI film is only 15 μm-thick (ca.~ 1/10 of inorganic polarizers), tough, and flexible, which leads to great advantages in processability and mass-production required for the applications in micro-optics and waveguide devises.

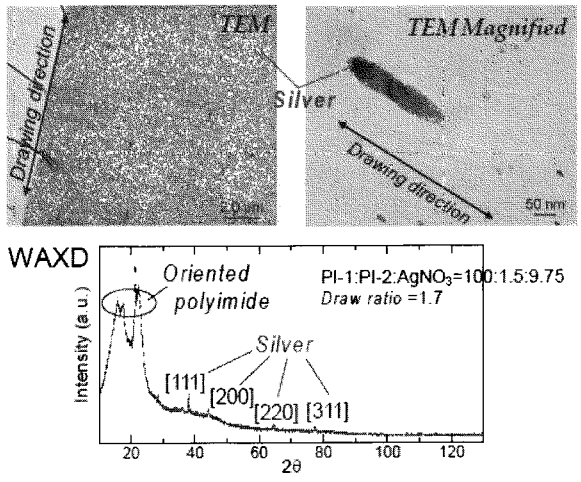

Fig.7 Cross-sectional TEM micrograph of silver doped PI film (left), the magnified image of a typical silver nano-rod (right), and WAXD pattern (bottom).

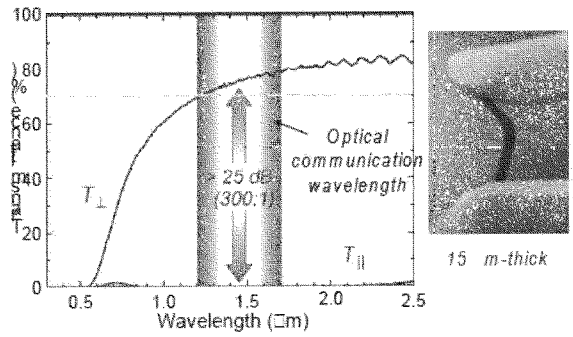

Fig.8 Polarized optical transmission spectra of a silver-doped PI film prepared under the optimized curing and drawing condition, and its appearance.

Summary

Organic/inorganinc PI nanohybrid materials having optical functionalities, such *a*) high refractive indices (n=1.81), *b*) low refractive indices (n=1.47), *c*) controlled thermo-optical property ($|dn/dT|$>350 ppm/K) and its anisotropy, and *d*) high polarizing property (dichroic ratio >500), have been developed by the nano-hybridization techniques based on the pyrolytic reactions (reduction, oxidation, and decomposition) of organo-soluble metallic precursors followed by spontaneous precipitation of metal/inorganic nanoparticles in solid PI films. This technique enables us to develop novel optical materials having a variety of optical functionality with maintaining the inherent excellent properties of PI films.

Acknowledgement : The author acknowledges that the reviewed results have been obtained by the fruitful collaborations with Prof. Mitsuru Ueda, Yuji Shibasaki, Sho-ichi Matsuda, Yoshiharu Terui, Akiko Matsumura, Yasuo Suzuki, Atsuhisa Suzuki, Yasuhiro Nakamura (*Tokyo Tech*), Jin-gang Liu (*present: The Chinese Academy of Science*), and Claudio A. Terraza (*present: Pontificia Univ. Catolica de Chile*).

References

1) C. T. Sullivan, *Proc. SPIE*, **994**, 92 (1988).
2) R. Reuter, H. Franke, and C. Feger, *Applied Optics*, **27**, 4565 (1988).
3) H. Franke, D. Wagner, T. Kleckers, R. Reuter, H. V. Rohitkumar, and B. A. Blech, *Applied Optics.*, **32**, 2927 (1993).
4) G. Hougham, P. E. Cassidy, K. Johns, and T. Davidson, eds. "*Fluoropolymers 1: Synthesis*" and "*Fluoropolymers 2: Properties*", Kluwer Academic/ Plenum Publishers, New York (1999).
5) S. Ando, *J. Photopolym. Sci. Technol.*, **17**, 219 (2004).
6) L. Zimmermann, M. Weibel, W. Caseri, U. W. Suter, and P. Walther, *Polym. Adv. Technol.*, **4**, 1 (1993).
7) M.Weibel, W. Caseri, U.W. Suter, H. Kiess, and E. Wehrli, *Polym. Adv. Technol.*, **2**, 1 (1991).
8) '*Hybrid Materials, Synthesis, Characterization, and Applications*', Ed.G. Kickelbick, WILEY-VCH, Weinheim (2007).
9) J.-G. Liu, Y. Nakamura, Y. Shibasaki, S. Ando, and M. Ueda, *Polym. J.*, **39**, 543 (2007).
10) J.-G. Liu, Y. Nakamura, Y. Shibasaki, S. Ando, M. Ueda, *Macromolecules*, **40**, 4614 (2007).
11) J.-G. Liu, Y. Nakamura, Y. Suzuki, Y. Shibasaki, S. Ando, and M. Ueda, *Macromolecules*, **40**, 7902 (2007).
12) J.-G. Liu, Y. Nakamura, Y. Suzuki, Y. Shibasaki, S. Ando, and M. Ueda, *J. Polym. Sci. Part A, Polym Chem.*, **45**, 5606 (2007).
13) J.-G. Liu, Y. Nakamura, T. Ogura, Y. Shibasaki, S. Ando, and M. Ueda, *Chem. Mater.*, **20**, 273 (2008).
14) J.-G. Liu, Y. Shibasaki, S. Ando, and M. Ueda, *High Perform. Polym.*, **20**, 221 (2008).
15) J.-G. Liu, Y. Nakamura, C.A. Terraza, Y. Shibasaki, S. Ando, and M. Ueda, *Macromol. Chem. Phys.*, **209**, 195 (2008).
16) C.A. Terraza, J.-G. Liu, Y. Nakamura, Y. Shibasaki, S. Ando, and M. Ueda, *J. Polym. Sci., Part A: Polym. Chem.*, **46**, 1510 (2008).
17) Y. Suzuki, J.-G. Liu, Y. Nakamura, Y. Shibasaki, S. Ando, and M. Ueda, *Polymer J.*, **40**, 414 (2008).
18) Y. Suzuki, Y. Nakamura, S. Ando, and M. Ueda, *J. Photopoly. Sci. Technol.*, **21**, 131 (2008).
19) S. Ando, T. Fujigaya, and M. Ueda, *Jpn. J. Appl. Phys.*, **41**, L105 (2002).
20) S. Ando, T. Fujigaya, and M. Ueda, *J. Photopolym. Sci. Technol.*, **15**, 559 (2002).
21) S. Ando and M. Ueda, *J. Photopolym. Sci. Technol.*, **16**, 537 (2003).
22) T. Fujigaya, Y. Shibasaki, S. Ando, S. Kishimura, M. Endo, M. Sasago, and M. Ueda, *Chem. Mater.*, **15**, 1512 (2003).
23) S. Ando, *J. Photopolym. Sci. Technol.*, **19**, 351 (2006).
24) S. Ando, Y. Watanabe, and T. Matsuura, *Jpn. J. Appl. Phys. Part 1*, **41**, 5254 (2002).
25) S. Ando, A. Suzuki, Y. Nakamura, J.-G. Liu, and M. Ueda, *Proc. STEPI*, **8**, (2008) (*in press*).
26) S. Matsuda, Y. Urano, J.-W. Park, C.-S. Ha, S. Ando, *J. Photopolym. Sci. Technol.*, **17**, 241 (2004).
27) S. Fujihara, M. Tada, and T. Kimura, *Thin Solid Films*, **304**, 252 (1997), *ibid*, **389**, 227 (2001).
28) Y. Terui and S. Ando, *Appl. Phys. Lett.*, **83**, 4755 (2003).
29) Y. Terui and S. Ando, *J. Photopolym. Sci. Technol.*, **18**, 337 (2005).
30) Y. Terui and S. Ando, *Proc. SPIE*, **5724**, 336 (2005).
31) Y. Terui and S. Ando, *High Perform. Polym.*, **18**, 825 (2006).
32) A. Matsumura, Y. Terui, S. Ando, A. Abe and T. Takeichi, *J. Photopolym. Sci. Technol.*, **20**, 167 (2007).
33) T. Sawada and S. Ando, *Chem. Mater.*, **10**, 3368 (1998).
34) T. Sawada, S. Ando, and S. Sasaki, *Appl. Phys. Lett.*, **74**, 938 (1999).
35) S. Matsuda, S. Ando, and T. Sawada, *Electron. Lett.*, **37**, 706 (2001).
36) S. Matsuda and S. Ando, *Polym. Adv. Technol.*, **14**, 458 (2003).
37) S. Matsuda, Y. Yasuda, and S. Ando, *Adv. Mater.*, **17**, 2221 (2005).